inter.noise 2014
MELBOURNE AUSTRALIA
16-19 NOVEMBER

Application of stochastic wind model to investigate swishing characteristics of infrasound and low frequency noise from wind turbine

Gwang-Se Lee[1], Cheolung Cheong[2]

Pusan National University, Republic of Korea

ABSTRACT

Swishing characteristics of infrasound and low frequency noise radiating from a modern large horizontal-axis wind turbine are investigated by employing stochastic wind model to reproduce realistic incident wind conditions upstream of the wind turbine. The stochastic wind is generated through the superposition of colored noise on mean wind profile. The colored noise is computed by applying low-pass filter to white noise. The filter represents the geometric and atmospheric conditions around the target turbine. The wind profiles generated in this way are applied to compute aerodynamic response on blades of the wind turbine by using the XFOIL code. The computed airfoil response is finally incorporated to predict the infrasound and low frequency noise of the wind turbine by using the Lowson's acoustic analogy. When only the mean wind profile is applied, the swishing effects in the predicted time-frequency maps of the wind turbine noise are clearly identified. However, unsteadiness in the incident wind profile leads to more complex swishing characteristics, which are often found in the noise signals obtained from field measurements. This result implies that operational condition on site in which the wind turbine is installed needs to be taken into account to more accurately assess the sound quality of wind turbine noise due to its swishing.

Keywords: Wind turbine noise, Swishing noise, Lowson's acoustic analogy I-INCE Classification of Subjects Number(s): 14.5.4, 21.6.4

1. INTRODUCTION

Infrasound and low frequency (ILF) noises including their amplitude modulation are important characteristics of wind turbine noise, which are known to make it more annoying than other mechanical systems with similar overall noise levels. On the more, their long propagation into far field can lead to more complain from residents nearby. Despite abovementioned considerations, it is not easy to analyze ILF noise using the measured data because of the masking effects by background noise from unknown sources.

The goal of present study is to develop effective numerical methods to assess the ILF noise of wind turbines with its swishing characteristics. The proposed method is based on the Lowson's acoustic analogy combined with stochastic wind profile model. Unsteady variation in wind speed profiles computed using the stochastic model are fed into the XFOIL code (2) to compute aerodynamic response on blade sections of wind turbines. Based on Lowson's acoustic analogy with the source data modelled by the aerodynamic responses, the ILF noises from a horizontal-axis wind turbine of 2 MW are predicted. In particular, the amplitude modulation of the noise corresponding to swishing of the ILF is examined in detail.

In Section 2, Lowson's acoustic analogy and the stochastic wind model are briefly introduced. In Section 3, the main results and the related discussions are provided.

[1] gs.lee@pusan.ac.kr
[2] ccheong@pusan.ac.kr

2. Methodology

2.1 Lowson's acoustic analogy

Lowson derived formula to describe sound field caused by arbitrary moving singularity by extending Lighthill's acoustic analogy for a source in rectilinear motion as (3):

$$\rho_t^{`} = \frac{1}{4\pi a_0^2}\left[\frac{(x_i - y_i)}{a_0 r^2(1-M_r)^2}\left\{\frac{\partial F_i}{\partial t} + \frac{F_i}{1-M_r}\frac{\partial M_r}{\partial t}\right\} + \frac{1}{r^2(1-M_r)^2}\left\{\frac{F_i(x_i - y_i)}{r}\left(\frac{1-M^2}{1-M_r}\right) - F_i M_i\right\}\right], \tag{1}$$

where a_0 is speed of sound, F_i is exerted force as source, M means Mach number of moving sources and r is the distance between a source and an observer. x_i and y_i represent locations of observer and source, respectively. The acoustic field corresponding to point loading sources in arbitrary motion is found to be composed of superposition of acoustic pressures represented by five terms: Doppler shift effects (1-M_r); unsteadiness of force, $\partial F_i/\partial t$; acceleration from source to observer, $\partial M_r/\partial t$; geometric(spherical) spreading of wave, $F_\text{i}(x_\text{i}$-$y_\text{i})/r$; convection of source, F_iM_i.

In order to apply the Lowson's analogy to predict ILF noise of wind turbines, firstly pressure distributions on the blade surface have to be computed. The pressure distributions on the blades of commercial wind turbine are computed with its operational conditions by using the XFOIL. Blade surface are discretized using finite elements and each element is converted as a moving force term of which the magnitude is obtained by multiplying the interpolated pressure at the center of the finite element times its area.

Aerodynamic noise from a small vertical wind turbines are predicted to validate the acoustic code developed using the Lowson's analogy. The flow fields around the vertical wind turbine are simulated by using the commercial code, Fluent (version 14.5). Then the computed fields are used as inputs to the acoustic code to predict acoustic pressure at far field. For comparison, the same acoustic computation is carried out using Ffwocs Williams and Hawking's (FW-H) equation provided in Fluent. Figure 1 compares the predicted sound pressure spectrum of both codes. It can be seen that the spectra predicted using the current code shows good agreement with that using the commercial code.

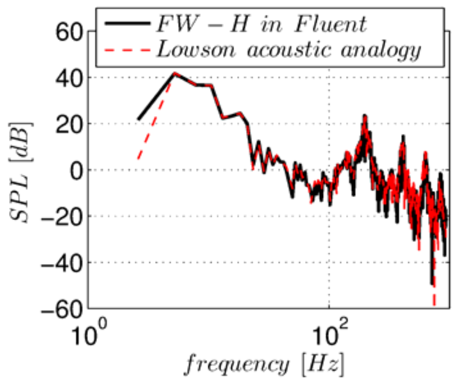

Fig. 1. Comparison of the predicted spectrum of acoustic pressure radiated from a small vertical wind turbine using Ffowcs Williams and Hawking's equation (in Fluent) and Lowson's analogy in the present code: observer's position is in the far-field, $r >> \lambda_{1st}$, where r is distance from the center of turbine to the observer and λ_{1st} is wavelength of first blade-passing frequency component.

2.2 Stochastic wind profile model

Most of previous studies have used mean wind profile to investigate wind turbine noise. Wind profiles were generally computed by using power or logarithmic law which describes distribution of wind speed along altitude. To reproduce more realistic conditions of wind incident to the wind turbine, stochastic wind model is applied. First, low pass filter is used to generate colored noise, and then unsteady wind speeds are generated by superposing the filtered wind speeds with quasi-steady one to simulate wind turbine performance in real time. The details about the stochastic model are described below.

The stochastic wind model consists of two components: quasi-steady wind speeds obtained from Van der Hoven's model and unsteady wind speeds computed by a stochastic model (4). The Van der Hoven's wind model is related to time scales of hours and days, which serves a role as the steady model in acoustic analysis since the longest time scale of acoustic is seconds. In this study, therefore, the mean wind profile along altitudes is computed using the Van der Hoven's model. The stochastic model generates wind speeds in time scales of seconds. Both wind speed models are functions of the parameters which can be determined from the environmental conditions in the site of wind turbines.

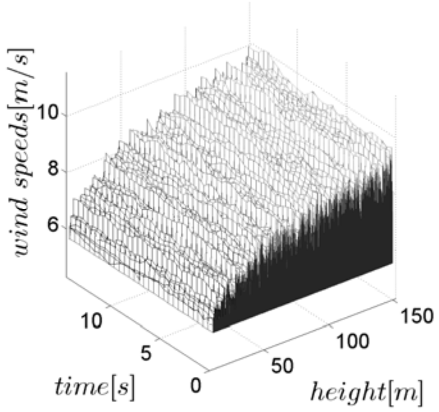

Fig. 2. Real-time wind profiles along height simulated using stochastic model.

In this study, the real time wind speed, v, involving the quasi-steady and the unsteady can be written in the following equation:

$$v(t) = V_z + \sigma_v v_t(t), \tag{2}$$

where V_z indicates the steady wind speed, v_t represents the unsteady speed and σ_v is a estimated standard deviation of steady wind speed in a given site. First, the steady wind speed, V_z, at the height, z, is computed using the power or logarithmic model. The logarithmic wind speed model in IEC 61400-11 is applied as written in the form (1):

$$V_s = V_z \left[\ln\left(\frac{z_{ref}}{z_{0ref}}\right) \ln\left(\frac{H}{z_0}\right) / \ln\left(\frac{H}{z_{0ref}}\right) \ln\left(\frac{z}{z_0}\right) \right], \tag{3}$$

where z_{ref} (=10 m) is the reference height, z indicates the height of an anemometer, H means the height of rotor center, z_0 is ground roughness length, which is 0.05 m in this study, $z_{0\mathrm{ref}}$(=0.05 m) is the reference roughness, and V_s is the standardized wind speed. Using Eq. (3) with V_z at a given altitude z, the mean wind speed is calculated. Next, by grossly following a procedure of Nichita et al., the unsteady wind speed is generated (4). In their study, the unsteady wind model are defined using colored noise as

$$v_t(t) = \int_0^t h(\tau) w(t-\tau) d\tau, \tag{4}$$

where $h(\tau)$ denotes impulse response of filters representing statistical characteristics of atmospheric inflow and $w(t)$ is white noise. The impulse response is expressed as

$$h(t) = \frac{2}{\pi} \int_0^\infty P(\omega) \cos(\omega t) d\omega, \tag{5}$$

where

$$P(\omega) = \mathrm{Re}\left[\frac{K_t}{(1 + j\omega T_f)^{5/6}} \right], \tag{6}$$

$$K_t \approx \sqrt{\frac{2\pi}{B\left(\frac{1}{2}, \frac{1}{3}\right)} \frac{T_f}{T_s}}, \tag{7}$$

$$T_f = \frac{T_L}{V_Z}. \tag{8}$$

where low pass filter, $P(\omega)$, is a function of parameters: the gain, K_t, the sampling period, T_s, a characteristic time scale, T_f, and atmospheric turbulent length scale, T_L. In this paper, an empirical formula is used to compute T_L with ground roughness condition as input parameter (5). Finally, the stochastic wind speed is obtained by multiplying the unsteady component, v_t (t), with estimated standard deviation, σ_v. The standard deviation can be experimentally estimated from the regression analysis of the wind speeds measured at a given site.

Aerodynamic computations are conducted at the time interval matching to one degree of rotation of the wind turbine. Therefore, 360 sets of real time wind profiles during single rotation of the wind turbine are generated prior to aerodynamic computations. Figure 2 describes typical time-varying wind profiles computed along altitudes.

3. Results

3.1 Noise map around wind turbine

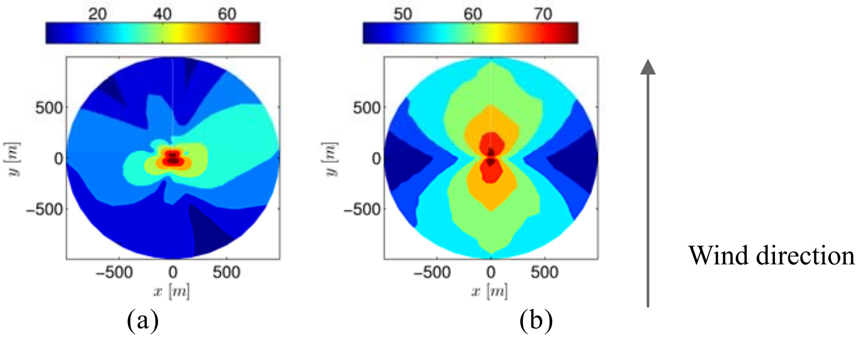

Fig. 3. Distribution of OASPL (below 50 Hz) around the wind turbine calculated using: (a) averaged wind profile; (b) stochastic wind profile.

Figure 3 shows distribution of the predicted overall sound pressure levels (OASPLs) on the ground near the wind turbine. For the case using averaged wind profile in Fig. 3(a), the distribution of the OASPLs is similar to quadrupole directivity and shows stronger levels in the right-hand side due to Doppler effects of rotating blades toward ground. This result can be understood using the classical acoustic theory on propeller noise (6). The directivity of SPLs calculated using the stochastic wind model, shown in Fig. 3 (b), shows dipolar pattern which is generally known to be characteristics of wind turbine noise where broadband noise components are dominant. It can be inferred from these results that unsteadiness of incident wind speeds generated the inflow broadband noise components in ILF range.

3.2 Swishing characteristics

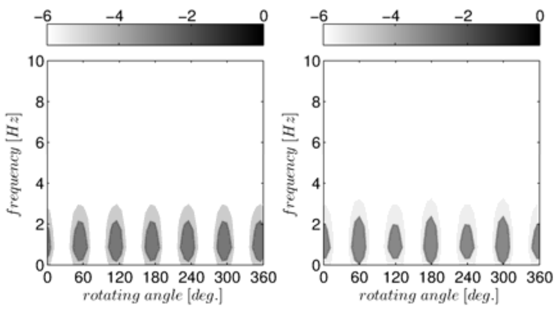

Fig. 4. Tim-frequency map of relative sound pressure level during one third cycle of rotor at given locations using averaged wind model:

(a) $x = 0.0$ m and $y = R_{IEC}$; (b) $x = R_{IEC}$ and $y = 0.0$ m.

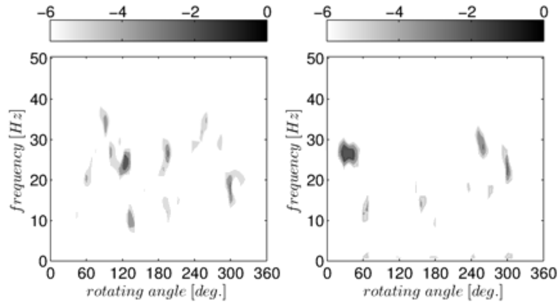

(a) (b)

Fig. 5. Tim-frequency map of relative sound pressure level during one third cycle of rotor at given locations using stochastic wind model:

(a) x = 0.0 m and $y = R_{IEC}$; (b) $x = R_{IEC}$ and y = 0.0 m.

In order to analyze swishing characteristics of the ILF noise of wind turbines, spectrograms of relative sound pressure levels predicted at two different receiver's locations are shown in Figs. 4 and 5. Short-time fast Fourier transform (FFT) is used to compute spectrogram with Hanning window of size corresponding to 32 samples and overlap ratio of 70%. Distances from hub to receiver's locations are the same, $R_{IEC}=h+r$, where h is the height of the turbine and r denotes the radius of rotor's blade. Cyclic period is assumed to be the same as the blade-passing period of the rotor. The amplitude modulation can be observed in the time-frequency maps computed using the short-time FFT for both cases using the averaged wind profile and the stochastic wind model.

When the averaged wind profile is applied, clearer modulation pattern in the low frequency range below 4 Hz can be identified in both locations. However, the modulation seems to be irregular with stronger high frequency components in the case using the stochastic model. This intermittent modulation may be due to unsteadiness of incident wind speeds. This result is believed to simulate real situation more closely, since irregular and intermittent acoustic modulation is often found in the measured wind turbine noise. This implies that unsteadiness in the incident wind speeds will lead to the complicated acoustic modulation. If sufficient acoustic data at given locations are measured and the averaging procedure is applied to this data, more regular modulation patterns can be identified just like the result shown in Fig. 5(a). This is similar to the beam-forming technique to find apparent cyclic noise source on the rotor plane (7).

4. CONCLUSIONS

Infrasound and low frequency noise radiating from the horizontal-axis wind turbine are investigated to analyze both its OASPLs and acoustic swishing characteristics by using the stochastic wind model combined with aerodynamic panel method of XFOIL and Lowson's acoustic analogy. Inflow noise radiating from the wind turbine predicted by applying stochastic wind model show dipolar directivity, while acoustic pressure computed with averaged wind model shows quadrupolar directivity which is typical results of BPF (blade-passing-frequency) noise from rotating machines. Time-frequency maps of sound pressure level are predicted at the locations in downwind and crosswind sides. Both maps show the swishing pattern. However, the predictions using the averaged wind speed profiles shows clearer swishing characteristics whereas those using the stochastic model looks more random. The latter seems to be closer to the measured data, which will be confirmed in a next study.

ACKNOWLEDGEMENTS

This research was supported by Basic Science Research Program through the National Research Foundation of Korea(NRF) funded by the Ministry of Science, ICT & Future Planning(NRF-2013R1A1A2012672), and also supported by the Human Resources Development program(No. 20134030200290) of the Korea Institute of Energy Technology Evaluation and Planning(KETEP) grant funded by the Korea government Ministry of Trade, Industry and Energy.

REFERENCES

1. IEC 61400-11:2002 Wind Turbines – Part 11: Acoustic noise measurement techniques, International Electrotechnical Commission, Geneva, Switzerland,.
2. M. Drela. XFOIL: An analysis and design system for low Reynolds number airfoils. In: Low Reynolds number aerodynamics. Berlin Heidelberg, Springer, 1989, p. 1-12.
3. M. V. Lowson. The sound field for singularities in motion. Proceedings of the Royal Society of London. Series A. Mathematical and Physical Sciences. 1965; 286(1407): 559-572.
4. C. Nichita, D. Luca, B. Dakyo and E. Ceanga. Large band simulation of the wind speed for real time wind turbine simulators. Energy Conversion, IEEE Transactions on. 2002; 17(4): 523-529.
5. W. J. Zhu. Modelling of noise from wind turbines. Mechenical Department, DTU, DK-2800, Lyngby, 2004.
6. M. Goldstein. Propeller noise: Gutin's theory. In: Aeroacoustics. New York, USA: McGraw-Hill Book Company; 1976, p. 153-171
7. G.-S. Lee, C. Cheong, S.-H. Shin and S.-S. Jung. A case study of localization and identification of noise sources from a pitch and a stall regulated wind turbine. Applied Acoustics. 2012; 73: 817-827.